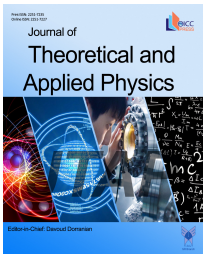

Volume 18, Issue 5, 182458 (1-13)

Journal of Theoretical and Applied Physics (JTAP)

https://dx.doi.org/10.57647/j.jtap.2024.1805.58

First principle investigation of the structural, electronic, optical, and elastic properties of Ba-based fluoroperovskite ($BaYF_3$; Y = Li, Na, K, and Rb) compounds

Hayder Muwafaq Ghazi*, Ali Hussain Reshak

Physics Department, College of Science, University of Basrah, Basrah, Iraq.

***Corresponding author:** haydermuwafaq94@gmail.com

Original Research

Received:
26 June 2024
Revised:
20 August 2024
Accepted:
23 August 2024
Published online:
30 October 2024

© The Author(s) 2024

Abstract:

The $BaYF_3$ (Y = Li, Na, K, and Rb) materials as cubic fluoro-perovskite compounds were examined by exploiting the full electron potential technique (FP-LAPW) and DFT through space of the Wien2k package to analyze their electronic and optical characteristics. The structural characteristics were determined through the generalized gradient approximation PBE-GGA functional, while the TB-mBJ functional was applied to enhance the calculation of electronic and optical characteristics. By substituting the cation Y from Li to Na, K, and Rb elements, the lattice constant experiences an increase, but the bulk modulus undergoes a drop. By studying the density of states and energy band structure, it is evident that $BaYF_3$ (Y = Li, Na, K, or Rb) exhibits a direct ($\Gamma-\Gamma$) energy band gap as insulator compounds. The obtained band gaps are 8.33 eV for $BaLiF_3$, 7.75 eV for $BaNaF_3$, 6.27 eV for $BaKF_3$, and 5.35 eV for $BaRbF_3$. The dielectric function and some connected optical characteristics, including refractive index, absorption coefficient, extinction coefficient, and reflectivity, have been evaluated in the $0-30$ eV energy range. Due to their excellent absorption and reflection capabilities in the UV spectrum, we prefer exploiting these compounds for optoelectronic applications, specifically in the UV region. Also, we have characterized the elastic constants (C_{11}, C_{12}, and C_{44}) of the perovskite $BaYF_3$ compounds and their corresponding mechanical parameters by using WC-GGA approximation.

Keywords: Fluoroperovskite; First principle investigation; Optical properties; Structural properties; Elastic properties

1. Introduction

Among various materials, the cubic perovskite family with ABX_3 crystal structure, especially fluoro-perovskite ABF_3, has garnered increasing attention due to their numerous valuable applications across several industries. These applications include renewable energy generation [1], spintronic applications [2], photovoltaic systems [3], coating materials [4], and fuel cells [5]. Arranging the atomic structure of floroperovskite ABF_3 compounds is created by exploiting several alkalies and alkaline earth metals as A and B cations, with fluorine serving as the anion [6, 7]. The vast perovskite family involving fluoroperovskite has received notice for its unique physical characteristics, including UV transparency, high electron mobility [8], dielectric property [9], piezoelectricity, and magnetism [10]. Fluoroperovskite solids have garnered major attention in the fields of lenses and semiconductors [11]. The main reason for using cubic perovskite in lenses is its low birefringence. These compounds exhibit a significant characteristic in the form of a broad energy band gap. These materials, with their limited absorption edges, can be utilized in the production of glass materials that efficiently transmit vacuum ultraviolet (VUV) and ultraviolet (UV) wavelengths [12].

Kohi et al. conducted an experimental study by using an extreme free electron laser (EUV-FEL) to excite crystals of $KMgF_3$ and $BaLiF_3$ compounds. They noted that the energy gaps of these substances were approximately 7.75

eV and 8.41 eV, respectively [13]. Theoretical analysis suggests that $BaLiF_3$, $CaLiF_3$, and $SrLiF_3$ possess highly favorable electronic and optical characteristics, leading them to be used as excellent candidates in optical devices [14]. Mubarak et al. discovered a significant and direct ($\Gamma-\Gamma$) band gap in $BaLiF_3$, $BaKF_3$, $BaRbF_3$, and $BaNaF_3$ fluoroperovskites by applying first principle calculations. They also observed notable anisotropic behavior at both high and low energy levels [15].

This study primarily investigates the electronic, structural, optical, and elastic characteristics of barium-based fluoroperovskite compounds, namely $BaYF_3$, with Y being Li, Na, K, and Rb. The band gap was estimated using DFT with PBE-GGA approximation, and to avoid the limitations of PBE-GGA, we have augmented calculations by using the recently updated Becke-Johnson (mBJ) functional. This ensures a close match between the calculated energy gap results and the experimental values. Also, mBJ is adopted to complete other optical parameters involving dielectric function with their related refractive index, absorption, extinction, and reflectivity. The purpose of this study is to offer reliable and precise predictions for the $BaYF_3$ compounds. To do this, we employed the approximations of the TB-mBJ (optical properties) and WC-GGA (elastic properties) in conjunction with the (FP-LAPW) method carried out through the space WIEN2K program. We would like to draw attention to some previous studies that have used the mBJ approximation to enhance band gap values compared to experimental values [16–21].

2. Computational method

The $BaYF_3$ crystal is analyzed as a cubic structure with the space group (221) pm-3m. The crystal geometry of the $BaYF_3$ compound is displayed in Figure 1. The Ba atom is positioned at the coordinates (0.0, 0.0, 0.0), whereas the Y atom (Li, Na, K, and Rb) is positioned at the coordinates (0.5, 0.5, 0.5), and the F atom is placed at the coordinates (0.5, 0.5, 0.0), (0.0, 0.5, 0.5), and (0.5, 0.0, 0.5). The geometrical relaxation was performed to adjust the locations of the atoms and minimize the forces acting on them (1 mRy/A). The PPE-GGA approximation has been incorporated into the WIEN2K program, applying the complete capabilities of the linearized augmented plane wave (FP-LAPW) method [22, 23]. The electronic structure and associated electronic characteristics were estimated using the relaxed geometry obtained by PPE-GGA. To provide accurate estimations of band gaps and optical characteristics, the latest modified Becke-Johnson (mBJ) potential was utilized [16]. The elastic calculations of $BaYF_3$ crystal were separately checked using the new form of GGA approximation, which was developed by Wu and Cohen (WC-GGA) [24]. The basis functions were created using a spherically symmetric potential within the spheres while remaining constant outside the spheres [23]. The value of RMT is selected to be 2.5, 2.0, 1.8, 1.95, 2.0, and 2.0 a.u. for Ba, F, Li, Na, K, and Rb atoms, respectively. The convergence of the total energy was achieved by expanding the basis functions up to a maximum value of RMT*K_{max} = 7.0 within crystal space. We were taken (−6 Ry) as an energy difference separating the core and valence states. The upper value for L was controlled to be L_{max} = 10, while G_{Max} was controlled by Fourier expansion up to 12 ($a.u^{-1}$) to reduce the charge density. A total of 3000 K-points are utilized for sampling the initial Brillouin zone in reciprocal space to compute the relaxation dynamics, electronic, and elastic properties. To achieve total energy convergence, the self-consistency convergence threshold is set to 0.0001 Ry.

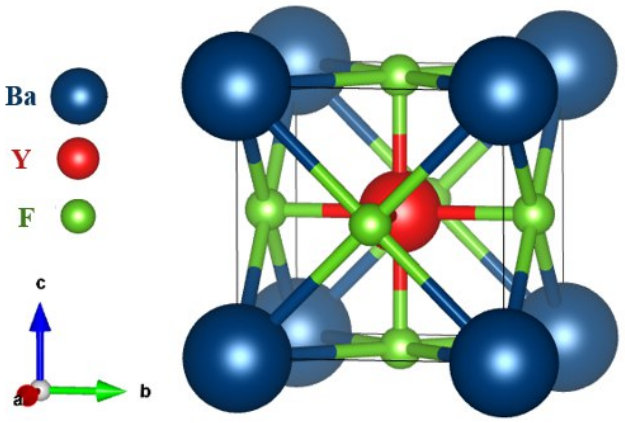

Figure 1. The atomic distribution within the unit cell of $BaYF_3$ compounds.

3. Results and discussion

3.1 Structural properties

Here, we examined $BaYF_3$'s cubic structure. The DFT calculations were conducted to complete the geometrical optimization by applying the PBE-GGA approach to accurately handle the exchange-correlation potential. The process of volume optimization starts by altering the volume, both decreasing and increasing it around the equilibrium volume. The changes in volume led to a consistent alteration in the internal energy for unit cell volume. Figure 2 exhibits the link between the changed volume and the related variations in total energy. The Murnaghan equation was employed to fit this plot and determined the values of the equilibrium state parameters such as lattice constant (a_o), bulk modulus (B_o) and derivative of bulk modulus ($\acute{B}_o$) for each compound [26]. These acquired parameters are compared to the previously conducted theoretical and available experimental studies, as detailed in Table 1. The equilibrium state yields lattice constants of 4.042 Å for $BaLiF_3$, 4.275 Å for $BaNaF_3$, 4.724 Å for $BaKF_3$, and 4.977 Å for $BaRbF_3$. The lattice constant of the $BaYF_3$ crystal increased as the Y position shifted from Li to Rb, respectively. However, the bulk modulus dropped in the same direction of shifting. The computed lattice constants revealed a remarkable agreement with earlier theoretical results [15, 27], while the lattice constant of $BaLiF_3$ was found to be higher than the experimental value [25]. We employed these optimum parameters to ascertain the optical and electronic characteristics of the bulk $BaYF_3$. Figure 1 indicates the crystal composition of the bulk $BaYF_3$ and the equilibrium constants (a_o, B_o, and $\acute{B}_o$) are given in Table 1.

3.2 Electronic properties

Analyzing the electronic characteristics is essential for obtaining an extensive knowledge of the structure and internal interactions within the atomic energy bands of materials and assessing the material efficiency for a specific application [28]. Therefore, we focused on comprehending the electronic characteristics of the bulk $BaYF_3$ (Y = Li, Na, K, and Rb).

We have analyzed the band structure, as shown in Figure 3. These calculations were performed using the optimal geometrical parameters listed in Table 1. We conducted band structure calculations using the PBE-GGA and enhanced by mBJ approximation, as indicated in Table 2. As mentioned previously, it may be concluded that mBJ enhances calculations of energy band gaps in comparison with PBE-GGA. We only utilized mBJ to analyze additional electronic properties, specifically TDOS and PDOS. The valence band (VB) maxima and conduction band (CB) minima of these compounds have their highest and lowest energy levels positioned at the gamma ($\Gamma-\Gamma$) point of the Brillion Zone, giving direct band gaps of about 6.74 eV, 6.16 eV, 4.48 eV, and 3.42 eV (PBE-GGA) and approximately 8.33 eV, 7.75 eV, 6.27 eV, and 5.35 eV (mBJ) for the $BaLiF_3$, $BaNaF_3$, $BaKF_3$, and $BaRbF_3$ compounds, respectively. The energy band gap values of $BaYF_3$ were consistently reduced as the Y-site atom was switched from Li to Rb. In this scenario, $BaLiF_3$ has a higher band gap value, whereas $BaRbF_3$ has a lower band gap value. Therefore, by substituting Y-site with Li, Na, K, and Rb atoms, the energy band gaps of the insulators under consideration can be modified in certain applications, making them very appropriate for employment in optoelectronic devices. The energy band gaps observed with PBE-GGA show a significant agreement with earlier theoretical research by PBE in reference [15]. Except for the $BaLiF_3$ compound, experimental data concerning the band gaps of these Ba (Na, K, and Rb) F_3 is currently unknown. The experimental band gap for $BaLiF_3$ is 8.41 eV [13], which is higher than our and prior mBJ and PBE theoretical computations [15, 27]. It is evident that the mBJ method significantly improves the calculated band gap for $BaLiF_3$, bringing it closer to the experimental value. Therefore, we anticipate that the mBJ method will also enhance the band gaps for $BaNaF_3$, $BaKF_3$, and $BaRbF_3$ compounds, making them more accurate compared to future experimental calculations than the PBE-GGA method. Consequently, we focused only on showing the findings generated by exploiting the mBJ approach.

Also, we only utilized mBJ to analyze additional electronic properties, specifically the total density of atomic states TDOS and the related partial contributions of the atom's orbital states PDOS. The valence states Ba-*s*, *p*, *d*, Li-*s*, *p*, and F-*s*, *p* were selected for the purpose of computing the TDOS and PDOS of each compound. The Fermi energy level was

Table 1. Some equilibrium parameters of $BaYF_3$ (Y = Li, Na, K, and Rb) were obtained from the structural relaxation process within the PBE-GGA approximation.

Compounds	a_o (Å)	B_o (GPa)	$\acute{B}_o$
$BaLiF_3$			
This work (PBE)	4.042	66.85	4.64
PBE [15]	4.04	66.46	5.17
PBE [15]	4.043	66.18	4.72
Exp [25]	3.996		
$BaNaF_3$			
This work (PBE)	4.275	52.77	4.53
PBE [15]	4.28	55.28	4.61
$BaKF_3$			
This work (PBE)	4.724	36.55	4.69
PBE [15]	4.72	37.48	4.51
$BaRbF_3$			
This work(PBE)	4.977	29.28	4.49
PBE [15]	4.96	31.72	4.66

Table 2. The determined energy band gaps (E_g) within TB-mBJ and PBE-GGA approaches for $BaYF_3$ compounds, where Y denotes the elements Li, Na, K, and Rb.

Compounds	E_g (eV)
$BaLiF_3$	
This work (mBJ)	8.33
This work (PBE)	6.74
MBJ [27]	8.26
PBE [27]	6.72
PBE [15]	6.8
Exp [13]	8.41
$BaNaF_3$	
This work (mBJ)	7.75
This work(PBE)	6.16
PBE [15]	6.1
$BaKF_3$	
This work (mBJ)	6.27
This work (PBE)	4.48
PBE [15]	4.6
$BaRbF_3$	
This work (mBJ)	5.35
This work (PBE)	3.42
PBE [15]	3.7

established at 0.0 eV, while the energy of the photon ranges from 15 to −30 eV. Figure 4 depicts the contributions of atoms, which construct the total density of states of $BaYF_3$. As we can see, the conduction bands of each compound are dominated by contributions of Ba atoms, whereas the valance bands are mainly dominated by the F atom in the energy spectrum from 0 to −5 eV near the Fermi level, with small contributions of Ba and Y atoms located from (−7) to (−30) eV. Figure 4 also shows the partial contributions of the atom's orbitals. As we see from the PDOS distribution of orbitals in Figure 4, the conduction bands of each compound are significantly dominated by Ba-5*d* with a small contribution of F-2*P* states, while the valence bands are mostly influenced by the F-2*p* state within the energy span from 0 to −5 eV with different small contributions of Y-*s*, *p*, Ba-*s*, *p*, and F-*s* states centered along the energy spectrum from −7 to −30 eV.

3.3 Optical characteristics

Investigation of the optical characteristics of $BaYF_3$ (X = Li, Na, K, and Rb) perovskite compounds enables us to accurately illustrate their various utilizations and probable applications in the optoelectronics field. Also from a deeper side, electronic transitions affect a material's optical characteristics and suitability for optical applications. There are two categories of electronic transitions that occur within solid materials. The first type is interband transfers. This phenomenon arises when charge carriers are stimulated to move from the valence band (VB) to the conduction band (CB). This transfer can occur through two methods: either directly or indirectly. The second category is intraband transitions, which refers to the movement of electrons within the same energy band in a material. In insulating materials, intraband transitions within the same bands are ignored, but transfers between the VB and CB are considered in the presence of high excitation energy [29, 30]. Depending on the improved band gap results as indicated above in Table 2, the TB-mBJ approach is adopted to obtain the optical characteristics of $BaYF_3$ compounds with energy (0–30) eV. The dielectric function $\varepsilon(\omega) = \varepsilon_1(\omega) + i\varepsilon_2(\omega)$ is employed to represent the connection between the electronic structure of the system and the tiny physical transitions occurring between energy bands. The real $\varepsilon_1(\omega)$ and the imaginary $\varepsilon_2(\omega)$ components are provided in the equations below [31].

$$\varepsilon_1(\omega) = 1 + \frac{2}{\pi} P \int_0^{\infty} \frac{\acute{\omega}\varepsilon_2(\acute{\omega})}{\acute{\omega}^2 - \acute{\omega}} d\acute{\omega} \tag{1}$$

$$\varepsilon_2(\omega) = \frac{2e^2}{\Omega\varepsilon_0} \sum_{K,V,C} |\langle \Psi_K^C | U, r | \Psi_K^V \rangle \square (E_K^C - E_K^V - E) \tag{2}$$

where Ψ_K^C and Ψ_K^V refer to the wave functions at a certain K in the CB and VB, respectively, Ω and e indicate the unit cell volume and the electronic charge, respectively, the unit vector U describes the polarization of the incoming electric field, E_K^C and E_K^V indicate the energy of electrons

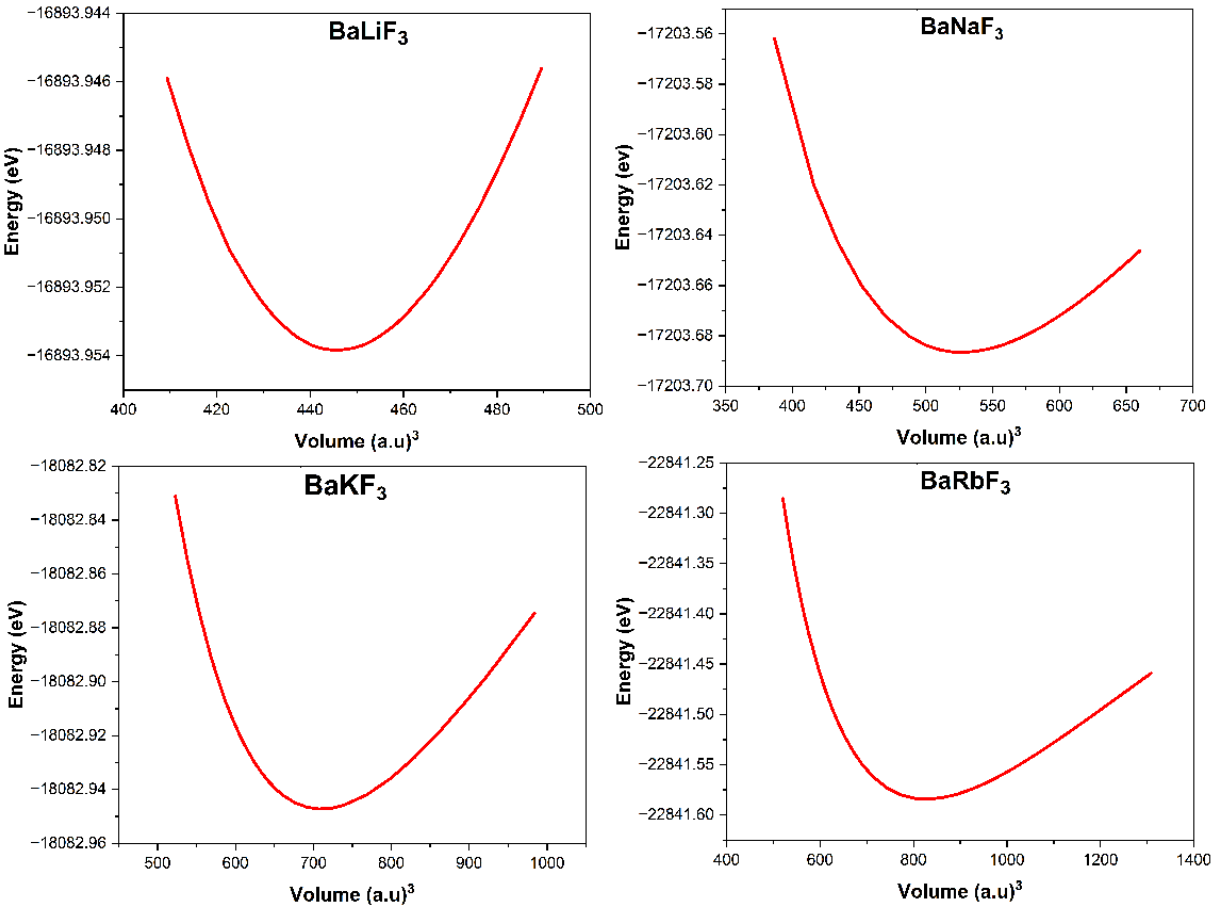

Figure 2. Optimization curves of $BaYF_3$ compounds, where Y denotes the elements Li, Na, K, and Rb.

at specific K-vectors in the CB and VB, and the delta function □ to keep energy and momentum conservation through the emission and absorption transitions of photons between electronic states.

The real component $\varepsilon_1(\omega)$ is related to the polarization of $BaYF_3$ compounds under the influence of incident light waves [32], as displayed in Figure 5 a. The spectra exhibit two notable positive peaks for each Y-site within $BaYF_3$. These peaks are positioned at 9.8 and 18.5 eV for Y = Li, 8.8 and 18.5 eV for Y = Na, 7.2 and 18.7 eV for Y = K, and 6.5 and 18.8 eV for Y = Rb. When the photon energy rises, the real part curve consistently decreases and reaches its minimum negative values with an arbitrary unit at about −3.16 at 19.8 eV, −3.68 at 19.5 eV, −4.36 at 19.4 eV, and

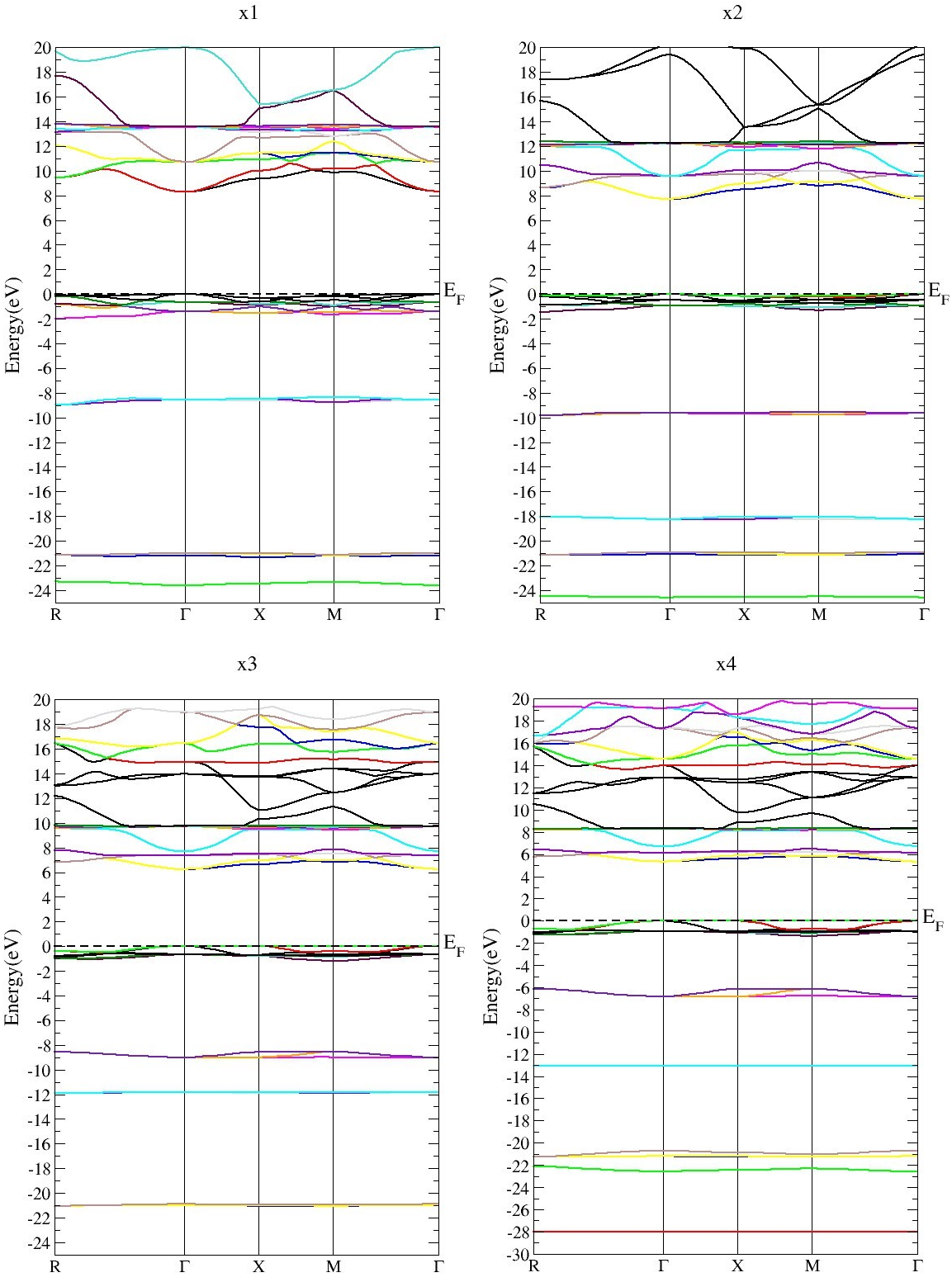

Figure 3. Band structure of the $BaYF_3$ compounds, where Y denotes the elements Li, Na, K, and Rb.

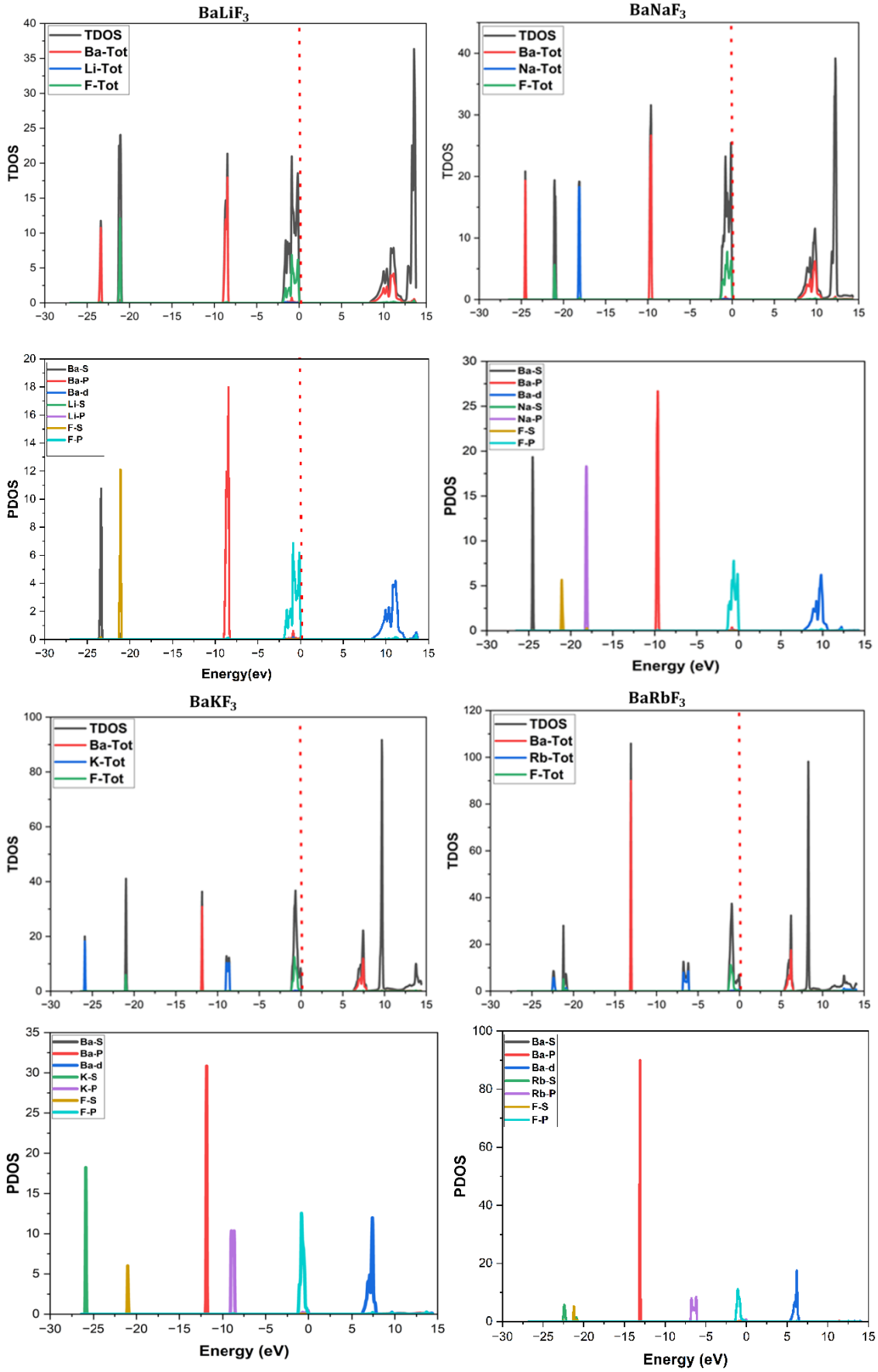

Figure 4. TDOS and PDOS of bulk $BaYF_3$ (Y = Li, Na, K, and Rb) within TB-mBJ approximation.

−4.44 at 19.38 for Y = Li, Na, K, and Rb, respectively. These negative values of $\varepsilon_1(\omega)$ related to the plasmonic vibrations of the insulating perovskite $BaYF_3$ compounds at high energy since these compounds lose their dielectric properties at these ranges of energy and become like semiconductors [3, 33]. At the zero frequency limits, the static dielectric function values for $BaLiF_3$, $BaNaF_3$, $BaKF_3$, and $BaRbF_3$ are approximately 1.95, 1.8, 1.8, and 1.79, respectively.

The dielectric function $\varepsilon_2(\omega)$ is concerned with the absorption (electronic transitions) in the $BaYF_3$ compounds when subjected to appropriate electromagnetic radiation [32]. As shown in Figure 5 b, the analysis of $\varepsilon_1(\omega)$ spectra for these compounds reveals noticeable peaks at 10.8 eV for $BaLiF_3$, 10.3 eV for $BaNaF_3$, 8 eV for $BaKF_3$, and 7 eV for $BaRbF_3$. The highest peaks of $\varepsilon_2(\omega)$ for these compounds are confined between 19 and 20 eV. These sharp peaks correspond to electronic transitions that occur between F-2*P* states located at the VB maxima and Ba-5*d* states at the CB minima. These transitions occur at the direct $(\Gamma-\Gamma)$ energy band gap. The threshold energies are around 4.8 eV for $BaLiF_3$, 4 eV for $BaNaF_3$, 2.9 eV for $BaKF_3$, and 2.5 eV for $BaRbF_3$, which corresponds with the expected values acquired by Mubarak [15].

Figures 5 a and 5 b show that at high energies, the $\varepsilon_1(\omega)$ and $\varepsilon_2(\omega)$ spectrums behave in opposing trends. This is because the Kramers-Kronig relationship provides a correlation between the $\varepsilon_1(\omega)$ and $\varepsilon_2(\omega)$ parts [34]. This means that when the value of the imaginary portion changes significantly, the real part also changes noticeably. In Figure 5 b, the sharp peaks of the $\varepsilon_2(\omega)$ at energy range from 19 to 20 eV mean the absorption and electronic transitions at their maximum states, which influence the $\varepsilon_1(\omega)$ to get negative values, indicating that an enormous amount of energy is dissipated, which leads to a reduction in the overall polarization and energy storage in these compounds [35].

The optical characteristics of $BaYF_3$ in the xx-direction, which include the refractive index $n(\omega)$, absorption coefficient $\alpha(\omega)$, extinction coefficients $K(\omega)$, and reflectivity $R(\omega)$, were studied employing the derived real and imaginary components, $\varepsilon_1(\omega)$ and $\varepsilon_2(\omega)$, of the dielectric function based on the following relation [31]:

$$n(\omega)=\frac{1}{\sqrt{2}}\sqrt{(\varepsilon_1^2(\omega)+\varepsilon_2^2(\omega))^{1/2}+\varepsilon_1(\omega)} \tag{3}$$

$$\alpha(\omega)=\frac{2\omega}{c}K(\omega) \tag{4}$$

$$K(\omega)=\frac{1}{\sqrt{2}}\sqrt{(\varepsilon_1^2(\omega)+\varepsilon_2^2(\omega))^{1/2}-\varepsilon_1(\omega)} \tag{5}$$

$$R(\omega)=\left|\frac{\sqrt{\varepsilon_1(\omega)+i\varepsilon_2(\omega)}-1}{\sqrt{\varepsilon_1(\omega)+i\varepsilon_2(\omega)}+1}\right| \tag{6}$$

The ($n(\omega)$: refractive index) is a fundamental parameter for calculating the degree of light refraction of $BaYF_3$ compounds, as shown in Figure 6 a. The evaluated ($n(0)$: static refractive index) is 1.4 for $BaLiF_3$, 1.34 for $BaNaF_3$, 1.34 for $BaKF_3$, and 1.33 for $BaRbF_3$, respectively. At low energies, the refractive index of $BaYF_3$ (Y = Li, Na, K, and Rb) compounds is most significant at 2.03 at 10.2 eV, 1.9 at 8.9 eV, 1.79 at 7.3 eV, and 1.73 at 6.57 eV, respectively. While at high energies, the maximum points are approximately 2.07 at 19.4 eV, 2.2 at 19.3 eV, 2.4 at 18.8 eV, and 2.56 at 18.9 eV, respectively. Due to interactions with electrons, photons are retarded as they enter a substance, resulting in $n(\omega)>1$. Photons are slowed to a greater extent as they pass through materials with a higher refractive index. $n(\omega)$ is often increased if the electron density of a compound is increased [6].

The absorption coefficient $\alpha(\omega)$ in Figure 6 b is calculated based on the dielectric function and provides information about the absorption threshold. It measures how much light with a certain energy can travel through a medium without getting absorbed. The imaginary component depicted in Figure 5 b corresponds to the absorption coefficient. The optical response of $BaLiF_3$ is recognized within the energy range of $8.3-30$ eV, while for $BaNaF_3$, it is recognized within the range of $7.75-30$ eV. Similarly, $BaKF_3$ exhibits an optical response in the range of $6.27-30$ eV, and $BaRbF_3$ shows an optical response in the range of $5.35-30$

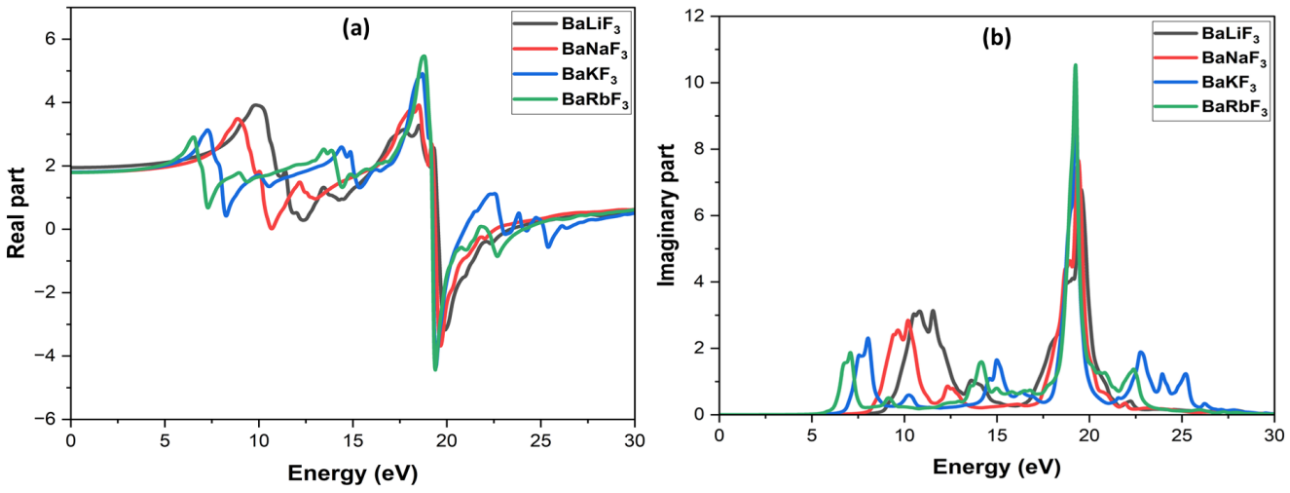

Figure 5. The determined (a) real and (b) imaginary parts of $BaYF_3$ compounds, where Y denotes the elements Li, Na, K, and Rb.

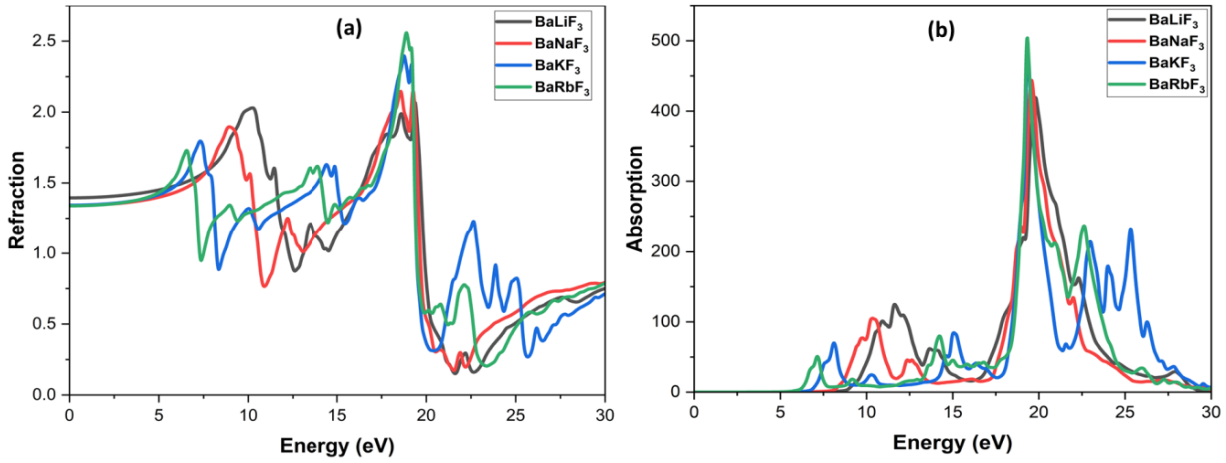

Figure 6. The determined (a) refraction index and (b) absorption coefficient of $BaYF_3$ compounds, where Y denotes the elements Li, Na, K, and Rb.

eV. It is worth noting that these materials do not exhibit any optical response below the respective band gap values of 8.3 eV, 7.75 eV, 6.27 eV, and 5.35 eV. These compounds exhibit their highest sensitivity at an energy range of $19-20$ eV. These findings indicate that $BaYF_3$ perovskites have the possibility of being optoelectronic devices in the UV region of the radiation spectrum.

The behavior of the extinction coefficient $K(\omega)$ in Figure 7 a and the spectrum of $\varepsilon_2(\omega)$ in Figure 5 b show a similar trend. The highest peaks of $K(\omega)$ exist as follows: 2.09 at 19.76 eV, 2.23 at 19.57 eV, 2.48 at 19.36 eV, and 2.57 at 19.33 eV for Y = Li, Na, K, and Rb, respectively. These values correspond to the real $\varepsilon_1(\omega)$ values at zero frequency. However, it should be noted that they exceed values generated by PBE-GGA calculations, as mentioned in reference [15]. The reflectivity $R(\omega)$ characterizes the surface's capacity to reflect the incoming electromagnetic radiation. Results exhibited in Figure 7 b indicate that the reflectivity of $BaYF_3$ compounds reaches its maximum peaks at low energies $(0-12$ eV) at around 10% and 19%. On the other hand, the lowest reflectivity values for $BaLiF_3$ are located at about $13-15.5$ eV, $11.4-14$ eV for $BaNaF_3$, $7.5-8.5$ eV for $BaNaF_3$, and for $BaRbF_3$, they fell within $8.5-11$ eV energy range. The reflectance spectrum of these compounds exhibits the greatest peaks as we move toward the UV spectrum at high energies, specifically about 71% for $BaLiF_3$, 63% for $BaNaF_3$, 61% for $BaKF_3$, and 56% for $BaRbF_3$. When the real part $\varepsilon_1(\omega)$ starts to display negative values, as shown in Figure 5 a, the reflectivity spectrum reaches its highest points, since the negative values indicate that the materials are reflecting all incident electromagnetic waves [39].

3.4 Elastic properties

The elastic characteristics of $BaYF_3$ compounds were checked by calculating the elastic constants (ECs) by adopting the WC-GGA functional. The ECs C_{ij} play a vital function in describing the mechanical features of a substance, clarifying how it undergoes deformation when subjected to stress and subsequently recovers its original position after stress release [40]. It is commonly known that cubic crystals are identified by three unique elastic constants, denoted as

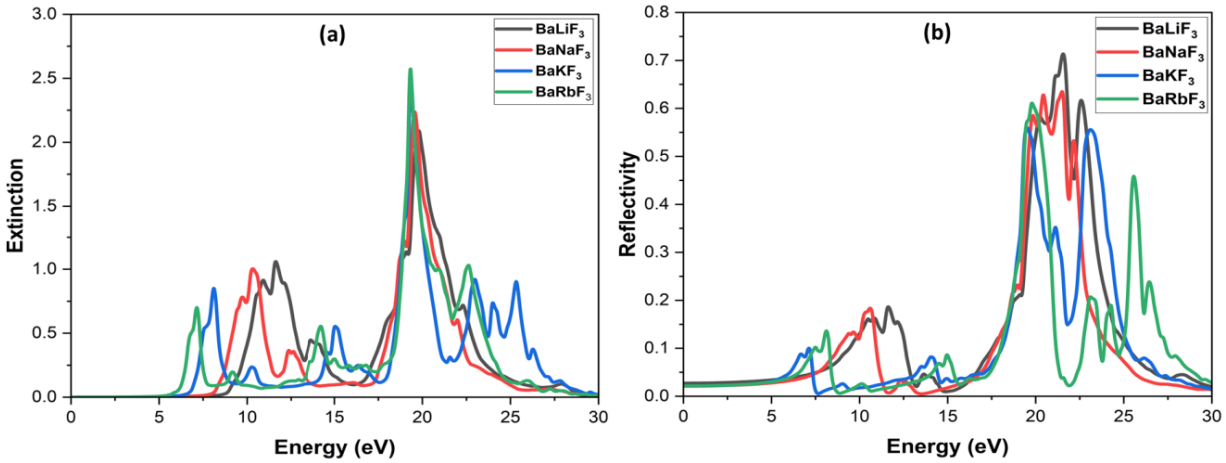

Figure 7. The determined (a) extinction coefficient and (b) reflectivity of $BaYF_3$ compounds, where Y denotes the elements Li, Na, K, and Rb.

(C_{ij}; where $ij = 11$, 22, and 44). The C_{ij} values in a cubic crystal are limited by constraints imposed by the demands of mechanical stability [41].

$C_{11}+2C_{12}>0$; $C_{11}-C_{12}>0$; $C_{11}>0$; $C_{44}>0$

The above requirements are achieved by the estimated C_{ij} outcomes in Table 3, which means that the perovskite $BaYF_3$ with (Y = Li, Na, K, and Rb) are mechanically stable. The C_{11} value for $BaLiF_3$ is 138.72 GPa, and 144.75 GPa for $BaNaF_3$ which are higher than the values of $BaKF_3$ and $BaRbF_3$. Thus, $BaLiF_3$ and $BaNaF_3$ are harder compared with other compounds. Depending on C_{11} values, the hardness of the $BaYF_3$ crystal decreases as we substitute the Y-site from Li to Rb. As possible as we know, there are no reported C_{ij} values that can be compared to our data, except for $BaLiF_3$, which both theoretical and experimental previous data are explained in Table 3. There are many elastic properties connected with C_{ij} of the materials that can be determined from Voigt-Reuss-Hill equations as outlined below [3, 42].

$$\text{Bulkmodulus}(B) = \frac{1}{3}(C_{11}+2C_{12}) \tag{7}$$

$$\text{Young'smodulus}(Y) = \frac{9BG}{G+3B} \tag{8}$$

$$\text{Shearmodulus}(G) = \frac{1}{2}(G_R+G_V) \tag{9}$$

$$\text{Anistropyratio}(A) = \frac{2C_{44}}{C_{11}-C_{12}} \tag{10}$$

$$\text{Poisson'sratio}(\upsilon) = \frac{3B-2G}{2(G+3B)} \tag{11}$$

Table 3 provides elastic parameters computed for $BaYF_3$ compounds and related elastic properties, which are calculated using Eqs. (7) - (11). The bulk modulus "B" gives an insight into the compound's resistance to volume changes. According to Table 3, the bulk modulus of $BaLiF_3$ is 77.15 GPa, 61.89 GPa for $BaNaF_3$, 40.69 GPa for $BaKF_3$, and 34.77 GPa for $BaRbF_3$. The structures of $BaLiF_3$ and $BaNaF_3$ compounds have a higher bulk modulus, indicating that they are less compressible than other compounds. There is a clear distinction between B values, which are calculated from C_{ij} and B_o values, which are derived from the Murnaghan equation in Table 1. This discrepancy arises because different approximations are used, specifically WC-GGA for elastic characteristics and GGA-PBE for structural properties. Young's modulus (Y) is a reliable measure to characterize a material's stiffness. A higher value of stiffness correlates to an increased level of rigidity for a specific material [43]. Based on the current findings of Y, we can conclude that $BaLiF_3$ and $BaNaF_3$ are stiffer than $BaKF_3$ and $BaRbF_3$. The toughness of the structure is represented by the shear modulus (G). As we see from the results in Table 3, $BaLiF_3$ is the hardest material, having a shear modulus of 46.99 GPa, compared with other compounds. This indicates that the $BaLiF_3$ compound has significant resistance to deformation. The induction of microcracks in solids is closely connected to the elastic anisotropy of crystals, which carries substantial implications for the engineering analysis of materials [44]. The anisotropy nature of $BaYF_3$ compounds is determined through the anisotropy factor (A), since compounds with $A = 1$ are completely isotropic, whereas $1 > A > 1$ indicates anisotropy. This led us to know that all our compounds show elastic anisotropy, but $BaLiF_3$ is more anisotropic than $BaNaF_3$, $BaKF_3$, and $BaRbF_3$ compounds [42]. Using Poisson's ratio (υ), ductile and brittle compounds were separated according to the value 0.26. Material getting a "υ" value lower than 0.26 is brittle, and vice versa [45]. Table 3 reveals that "υ" for $BaLiF_3$

Table 3. Results of elastic constants C_{ij}, bulk modulus, Young's modulus, and shear modulus (in GPa) and (anisotropic ratio, Poisson's ratio, and Pugh's ratio) of $BaYF_3$ (Y = Li, Na, K, and Rb) compounds.

Compounds	C_{11}	C_{12}	C_{44}	B	Y	G	A	υ	B/G
$BaLiF_3$									
This work	138.72	46.37	47.56	77.15	117.18	46.99	1.03	0.246	1.64
Theoret [36]	118.88	42.76	43.19	68.14	102.57	41.06	1.14	0.25	1.66
Theoret [37]	134.0	45.4	46.5	74.9		45.6			
Theoret [38]	163.84	50.81	60.02	88.84					
Exp [25]	130	46.5	48.7	79		45.9			
$BaNaF_3$									
This work	144.75	20.47	19.85	61.89	81.93	32.02	0.32	0.558	1.93
$BaKF_3$									
This work	115.16	3.46	0.87	40.69	33.15	12.15	0.015	0.364	3.35
$BaRbF_3$									
This work	101.53	1.4	8.61	34.77	48.28	19.03	0.17	0.269	1.83

is 0.246, 0.558 for $BaNaF_3$, 0.364 for $BaKF_3$, and 0.269 for $BaRbF_3$, indicating ductility for each compound except $BaLiF_3$, which appears to have a brittle nature. Pugh's ratio (B/G) is also a vital measure for assessing the brittleness and ductility of $BaYF_3$ compounds. It demonstrates ductility when the B/G ratio is greater than 1.75 and brittleness when the B/G ratio is lower than 1.75 [46]. The results gathered from the examination of perovskites $BaYF_3$ by Pugh's ratio are 1.64 for $BaLiF_3$, 1.93 for $BaNaF_3$, 3.35 for $BaKF_3$, and 1.83 for $BaRbF_3$. This means that $BaLiF_3$ is brittle, while $BaNaF_3$, $BaKF_3$, and $BaRbF_3$ compounds appear to have ductile behavior, which provides evidence of their ability to deform without breaking under external strain. As indicated in Table 3, our elastic results of $BaLiF_3$ appear to have good convergence with experimental and some other theoretical studies.

4. Conclusion

This study explores the structural, electronic, optical, and elastic characteristics of the barium-based fluoro-perovskite $BaYF_3$ (Y = Li, Na, K, or Rb) employing the TB-mBJ approximation. The bulk modulus lowers while the lattice constant increases throughout the transition from Li to Rb for the $BaYF_3$ crystal. These structural parameters demonstrate a reasonable correspondence with available theoretical studies. According to the electronic structure analysis, each of these four compounds showed an insulating property and a direct ($\Gamma - \Gamma$) band gap since changing elements from Li to Rb in the $BaYF_3$ crystal lowers the energy gap by displacing Ba-5d states to low energies. The refractive index and dielectric function with their real and imaginary components were studied. As we see, the main transitions occur between F-2P valence band states and Ba-5d conduction band states for each compound. The analysis of the absorption and reflectivity spectra of these materials revealed considerable values of absorption and reflectivity in the ultraviolet range. We also checked the elastic properties of $BaYF_3$ compounds by adopting WC-GGA functional. Based on the elastic data obtained, all compounds are stable. $BaLiF_3$ is brittle while other compounds are ductile; it is also found both $BaLiF_3$ and $BaNaF_3$ are harder than $BaKF_3$ and $BaRbF_3$, and all $BaYF_3$ compounds are elastic anisotropic.

Authors Contributions
Authors have contributed equally in preparing and writing the manuscript.

Availability of Data and Materials
The authors declare that the data supporting the findings of this study are available within the paper.

Conflict of Interests
The authors declare that they have no known competing financial interests or personal relationships that could have appeared to influence the work reported in this paper.

Open Access
This article is licensed under a Creative Commons Attribution 4.0 International License, which permits use, sharing, adaptation, distribution and reproduction in any medium or format, as long as you give appropriate credit to the original author(s) and the source, provide a link to the Creative Commons license, and indicate if changes were made. The images or other third party material in this article are included in the article's Creative Commons license, unless indicated otherwise in a credit line to the material. If material is not included in the article's Creative Commons license and your intended use is not permitted by statutory regulation or exceeds the permitted use, you will need to obtain permission directly from the OICC Press publisher. To view a copy of this license, visit https://creativecommons.org/licenses/by/4.0.

References

[1] R. Ullah and A. H. Reshak. "Pressure-dependent elasto-mechanical stability and thermoelectric properties of $MYbF_3$ (M = Rb , Cs) materials for renewable energy.". *International Journal of Energy Research*, **45**:1–13, 2021. DOI: https://doi.org/10.1002/er.6408.

[2] A. A. Pasha, H. Khan, M. Sohail, N. Rahman, R. Khan, and A. Ullah. "A computational first principle examination of the elastic, optical, structural and electronic properties of $AlRF_3$ (R = N, P) fluoroperovskites compounds.". *Molecules*, **28**, 2023. DOI: https://doi.org/10.3390/molecules28093876.

[3] S. A. Shah, M. Husain, N. Rahman, M. Sohail, and R. Khan. "Insight into the struvtural, electronic, elastic, optical, and magnetic properties of cubic fluoroperovskites ABF_3 (A = Tl , B = Nb , V) compounds: Probed by DFT.". *Nanomaterials*, **3**, 2022. DOI: https://doi.org/10.3390/ma15165684.

[4] Z. Jin, Y. Wu, S. Li, Q. Wu, S. Chen, and Y. Chen. "Results in physics electronic structure , elastic , optical and thermodynamic properties of cubic perovskite $NaBaF_3$ with pressure effects: First-principles calculations.". *Results Phys.*, **22**:103860, 2021. DOI: https://doi.org/10.1016/j.rinp.2021.103860.

[5] M. H. Benkabou, M. Harmel, A. Haddou, A. Yakoubi, N. Baki, and R. Ahmed. "Structural , electronic , optical and thermodynamic investigations of $NaXF_3$ (X = Ca and Sr): First-principles calculations.". *Nanoscale*, **56**:131–144, 2018. DOI: https://doi.org/10.1016/j.cjph.2017.12.008.

[6] W. Ullah, R. Nasir, M. Husain, N. Rahman, and H. Ullah. "Revealing the remarkable structural, electronic, elastic, and optical properties of Zn-based fluoroperovskite $ZnXF_3$ (x = Sr, Ba) employing DFT. ". *Indian J. Phys.*, **3**, 2024. DOI: https://doi.org/10.1007/s12648-024-03146-y.

[7] N. Chouit, S. A. Korba, M. Slimani, H. Meradji, S. Ghemid, and R. Khenata. "First-principles study of the structural, electronic and thermal properties of $CaLiF_3$. ". *Phys. Scr.*, **88**:139–153, 2013. DOI: https://doi.org/10.1088/0031-8949/88/03/035702.

[8] J. Zhang, Y. Chen, S. Chen, J. Hou, R. Song, and Z. F. Shi. "Electronic structure, mechanical, optical and thermodynamic properties of cubic perovskite $InBeF_3$ with pressure effects: First-principles calculations.". *Results Phys.*, **50**:106590, 2023. DOI: https://doi.org/10.1016/j.rinp.2023.106590.

[9] M. R. Kabli, J. ur Rehman, M. Bilal Tahir, M. Usman, A. Mahmood Ali, and K. Shahzad. "Structural, electronics and optical properties of sodium based fluoroperovskites $NaXF_3$ (X = Ca, Mg, Sr and Zn): First principles calculations.". *Phys. Lett. Sect. A Gen. At. Solid State Phys.*, **412**:127574, 2021. DOI: https://doi.org/10.1016/j.physleta.2021.127574.

[10] J. ur Rehman, M. Usman, M. B. Tahir, and A. Hussain. "First-principles calculations to investigate structural , electronic and optical properties of Na based fluoroperovskites $NaXF_3$ (X = Sr, Zn). ". *Solid State Commun.*, **334–335**:114396, 2021. DOI: https://doi.org/10.1016/j.ssc.2021.114396.

[11] T. N. Ishimatsu, N. T. Erakubo, H. M. Izuseki, Y. K. Awazoe, and D. A. P. Awlak. "Band structures of perovskite-like fluorides for vacuum-ultraviolet-transparent lens materials.". *Japanese Journal of Applied Physics*, **41**:10–13, 2002. DOI: https://doi.org/10.1143/JJAP.41.L365.

[12] M. Usman, J. ur Rehman, and M. B. Tahir. "Screening of ABF_3 fluoroperovskites by using first-principles calculations.". *Solid State Commun.*, **369**:1–6, 2023. DOI: https://doi.org/10.1016/j.ssc.2023.115198.

[13] K. Yamanoi, R. Nishi, K. Takeda, Y. Shinzato, M. Tsuboi, and M. Viet. "Perovskite fluoride crystals as light emitting materials in vacuum ultraviolet region.". *Opt. Mater. (Amst).*, **36**:769–772, 2014. DOI: https://doi.org/10.1016/j.optmat.2013.11.023.

[14] A. A. Mousa, N. T. Mahmoud, and J. M. Khalifeh. "The electronic and optical properties of the fluoroperovskite $XLiF_3$ (X = Ca, Sr, and Ba) compounds.". *Comput. Mater. Sci.*, **79**:201–205, 2013. DOI: https://doi.org/10.1016/j.commatsci.2013.06.016.

[15] A. A. Mubarak and A. A. Mousa. "The electronic and optical properties of the fluoroperovskite $BaXF_3$ (X = Li, Na, K, and Rb) compounds.". *Comput. Mater. Sci.*, **59**:6–13, 2012. DOI: https://doi.org/10.1016/j.commatsci.2012.02.020.

[16] F. Tran and P. Blaha. "Accurate band gaps of semiconductors and insulators with a semilocal exchange-correlation potential. ". *Phys. Rev. Lett.*, **102**:5–8, 2009. DOI: https://doi.org/10.1103/PhysRevLett.102.226401.

[17] A. H. Reshak. "Specific features of electronic structures and optical susceptibilities of molybdenum oxide.". *RSC Adv.*, **5**:22044–22052, 2015. DOI: https://doi.org/10.1039/c5ra00081e.

[18] A. H. Reshak, H. Huang, H. Kamarudin, and S. Auluck. "Alkali-metal/alkaline-earth-metal fluorine beryllium borate NaSr3Be3B3O9F4 with large nonlinear optical properties in the deep-ultraviolet region.". *J. Appl. Phys.*, **117**, 2015. DOI: https://doi.org/10.1063/1.4913693.

[19] J. A. Abraham, R. Sharma, V. Srivastava, and A. Ibrahim. "Insight into structural stability, electronic, optical and thermoelectric properties of the inverse perovskite Na_3SCl compound from first-principles study.". *Mater. Sci. Eng. B*, **301**:117184, 2024. DOI: https://doi.org/10.1016/j.mseb.2024.117184.

[20] S. Tariq, A. O. Alrashdi, A. Al Bahir, and S. M. Sohail. "DFT insights into $LaFeO_3$ with Mn substitution: A promising path to energy-efficient magneto-optical applications.". *J. Comput. Chem.*, **45**:843–854, 2024. DOI: https://doi.org/10.1002/jcc.27286.

[21] G. Ayub, A. Rauf, M. Husain, A. Algahtani, and V. Tirth. "Investigating the physical properties of thallium-based ternary $TlXF_3$ (X = Be, Sr) fluoroperovskite compounds for prospective applications.". *ACS Omega.*, **8**:17779–17787, 2023. DOI: https://doi.org/10.1021/acsomega.3c00549.

[22] K. Li, L. Luo, Y. Zhang, W. Li, and Y. Hou. "Tunable luminescence contrast in photochromic ceramics (1-X)Na 0.5 Bi 0.5 TiO_3-xNa 0.5 K 0.5 NbO_3:0.002Er by an electric field poling.". *ACS Appl. Mater. Interfaces*, **10**:41525–41534, 2018. DOI: https://doi.org/10.1021/acsami.8b15784.

[23] K. Schwarz and P. Blaha. "Solid state calculations using WIEN2k. ". *Comput. Mater. Sci.*, **28**: 259–273, 2003. DOI: https://doi.org/10.1016/S0927-0256(03)00112-5.

[24] Z. Wu and R. E. Cohen. "More accurate generalized gradient approximation for solids.". *Phys. Rev. B - Condens. Matter Mater. Phys.*, **73**, 2006. DOI: https://doi.org/10.1103/PhysRevB.73.235116.

[25] A. Boumriche, J. Y. Gesland, A. Bulou, J. L. Fourquet, and B. Hennion. "Structure and dynamics of the inverted perovskite $BaLiF_3$. ". *Solid State Communications*, **91**:125–128, 1994. DOI: https://doi.org/10.1016/0038-1098(94)90268-2.

[26] C. Ambrosch-Draxl and J. O. Sofo. "Linear optical properties of solids within the full-potential linearized augmented planewave method. ". *Comput. Phys. Commun.*, **175**:1–14, 2006. DOI: https://doi.org/10.1016/j.cpc.2006.03.005.

[27] B. G. Yalcin, B. Salmankurt, and S. Duman. "Investigation of structural, mechanical, electronic, optical, and dynamical properties of cubic $BaLiF_3$, $BaLiH_3$, and $SrLiH_3$.". *Mater. Res. Express*, **3**, 2016. DOI: https://doi.org/10.1088/2053-1591/3/3/036301.

[28] L. Celestine, R. Zosiamliana, L. Kima, B. Chttri, Y. T. Singh, S. Gurung, N. S. singh, and A. Laref. "Hybrid-DFT study of halide perovskites, an energy-efficient material under compressive pressure for piezoelectric applications.". *J. Phys. Condens. Matter*, **39**, 2024. DOI: https://doi.org/10.1088/1361-648X/ad443e.

[29] Y. Wang and W. Dou. "Interband and intraband transitions, as well as charge mobility in driven two-band model with electron phonon coupling.". *arXiv:2406.17817*, :1–8, 2024. DOI: https://doi.org/10.48550/arXiv.2406.17817.

[30] B. Bakri, Z. Driss, S. Berri, and R. Khenata. "First-principles investigation for some physical properties of some fluoroperovskites compounds ABF_3 (A = K, Na; B = Mg, Zn). ". *Indian J. Phys.*, **91**:1513–1523, 2017. DOI: https://doi.org/10.1007/s12648-017-1055-6.

[31] H. Zitouni, N. Tahiri, O. El Bounagui, and H. Ez-Zahraouy. "How the strain effects decreases the band gap energy in the $CsPbX_3$ perovskite compounds?". *Phase Transitions*, **93**:455–469, 2020. DOI: https://doi.org/10.1080/01411594.2020.1746964.

[32] Shakeel, A. H. Reshak, S. Khan, A. Laref, G. Murtaza, and J. Bila. "Pressure induced physical variations in the lead free fluoropervoskites XYF_3 (X = K, Rb, Ag; Y = Zn, Sr, Mg): Optical materials.". *Opt. Mater. (Amst).*, **109**:110325, 2020. DOI: https://doi.org/10.1016/j.optmat.2020.110325.

[33] L. Celestine, R. Zosiamliana, S. Gurung, S. R. Bhandari, A. Laref, S. Abdullaev, and D. P Rai. "A halide-based perovskite $CsGeX_3$ (X = Cl, Br, and I) for optoelectronic and piezoelectric applications.". *Adv. Theory Simulations*, **7**:1–12, 2024. DOI: https://doi.org/10.1002/adts.202300566.

[34] M. Alouani and J. Wills. "Calculated optical properties of Si, Ge, and GaAs under hydrostatic pressure.". *Phys. Rev. B - Condens. Matter Mater. Phys.*, **54**:2480–2490, 1996. DOI: https://doi.org/10.1103/PhysRevB.54.2480.

[35] N. Alfryyan, H. Khan, M. Sohail, R. Khan, and N. Rahman. "First-principles calculations to investigate structural, electrical, elastic and optical characteristics of BWF_3 (W = S and Si) fluoroperovskites.". *Results Phys.*, **52**:0–7, 2023. DOI: https://doi.org/10.1016/j.rinp.2023.106812.

[36] R. K. Pingak, S. Bouhmaidi, L. Setti, and B. Pasangka. "Structural, electronic, elastic, and optical properties of cubic $BaLiX_3$ (X = F, Cl, Br, or I) perovskites: An Ab-initio DFT study. ". *Indones. J. Chem.*, **23**:843–862, 2023. DOI: https://doi.org/10.22146/ijc.83261.

[37] Z. L. Lv, H. L. Cui, H. Wang, X. H. Li, and G. F. Ji. "Electronic and elastic properties of $BaLiF_3$ with pressure effects: First-principles study.". *Phys. Status Solidi Basic Res.*, **253**:1788–1794, 2016. DOI: https://doi.org/10.1002/pssb.201600094.

[38] S. A. Korba, H. Meradji, S. Ghemid, and B. Bouhafs. "First principles calculations of structural, electronic and optical properties of $BaLiF_3$.". *Comput. Mater. Sci.*, **44**:1265–1271, 2009. DOI: https://doi.org/10.1016/j.commatsci.2008.08.012.

[39] K. E. Babu, A. Veeraiah, D. T. Swamy, and V. Veeraiah. "First-principles study of electronic and optical properties of cubic perovskite CsSrF. ". *Mater. Sci. Pol.*, **30**: 359–367, 2012. DOI: https://doi.org/10.2478/s13536-012-0047-7.

[40] R. Khenata A. H. Reshak H. Rached, D. Rached and M. Rabah. "First-principles calculations of structural, elastic and electronic properties of Ni2MnZ (Z = Al, Ga and In) Heusler alloys. ". *Phys. Scr.*, **88**:139–153, 2013. DOI: https://doi.org/Phys. Status Solidi Basic Res., vol. 246, no. 7, pp. 1580–1586, 2009, DOI: 10.1002/pssb.200844400.

[41] A. Ayyaz, G. Murtaza, M. Umer, A. Usman, and H. H. Raza. "Structural, elastic, optoelectronic, and transport properties of Na-based halide double perovskites Na2CuMX6 (M = Sb, Bi, and X = Cl, Br) as renewable energy materials: A DFT insight.". *J. Mater. Res.*, **38**:4609–4624, 2023. DOI: https://doi.org/10.1557/s43578-023-01181-9.

[42] G. Murtaza, Hayatullah, R. Khenata, M. N. Khalid, and S. Naeem. "Elastic and optoelectronic properties of $RbMF_3$ (M = Zn, Cd, Hg): A mBJ density functional calculation.". *Phys. B Condens. Matter.*, **410**:131–136, 2013. DOI: https://doi.org/10.1016/j.physb.2012.10.024.

[43] Y. Liu, B. Liu, H. Xiang, Y. Zhou, and H. Nian. "Theoretical investigation of anisotropic mechanical and thermal properties of ABO_3 (A = Sr, Ba; B = Ti, Zr, Hf) perovskites.". *J. Am. Ceram. Soc.*, **101**:3527–3540, 2018. DOI: https://doi.org/10.1111/jace.15502.

[44] C. Kaderoglu, G. Surucu, and A. Erkisi. "The investigation of electronic, elastic and vibrational properties of an interlanthanide perovskite: $PrYbO_3$.". *J. Electron. Mater.*, **46**:5827–5836, 2017. DOI: https://doi.org/10.1007/s11664-017-5600-z.

[45] A. Habib, M. Husain, M. sajjad, N. Rahman, and R. Khan. "Insight into the exemplary physical properties of Zn-based fluoroperovskite compounds $XZnF_3$ (X = Al, Cs, Ga, In) employingAccurate GGA approach: A first-principle study.". *Materials*, **3**, 2022. DOI: https://doi.org/10.3390/ma15072669.

[46] N. Hasan, M. Arifuzzaman, and A. Kabir. "Structural, elastic and optoelectronic properties of inorganic cubic $FrBX_3$ (B 1/4 Ge, Sn; X 1/4 Cl, Br, I) perovskite: The density functional theory approach. ". *RSC Adv.*, **12**:7961–7972, 2022. DOI: https://doi.org/10.1039/d2ra00546h.